

Double Layer at the Pt(111)-Aqueous Electrolyte Interface: Potential of Zero Charge and Anomalous Gouy-Chapman Screening

Ojha, K.; Arulmozhi, N.; Aranzales, D.; Koper, M.T.M.

Citation

Ojha, K., Arulmozhi, N., Aranzales, D., & Koper, M. T. M. (2020). Double Layer at the Pt(111)-Aqueous Electrolyte Interface: Potential of Zero Charge and Anomalous Gouy-Chapman Screening. *Angewandte Chemie International Edition*, 59(2), 711-715. doi:10.1002/anie.201911929

Version: Publisher's Version

License: Creative Commons CC BY-NC 4.0 license

Downloaded from: https://hdl.handle.net/1887/85792

Note: To cite this publication please use the final published version (if applicable).







Metal-Electrolyte Interface

International Edition: DOI: 10.1002/anie.201911929 German Edition: DOI: 10.1002/ange.201911929

Double Layer at the Pt(111)-Aqueous Electrolyte Interface: Potential of Zero Charge and Anomalous Gouy-Chapman Screening

Kasinath Ojha, Nakkiran Arulmozhi, Diana Aranzales, and Marc T. M. Koper*

Abstract: We report, for the first time, the observation of a Gouy–Chapman capacitance minimum at the potential of zero charge of the Pt(111)-aqueous perchlorate electrolyte interface. The potential of zero charge of 0.3 V vs. NHE agrees very well with earlier values obtained by different methods. The observation of the potential of zero charge of this interface requires a specific pH (pH 4) and anomalously low electrolyte concentrations ($<10^{-3}$ M). By comparison to gold and mercury double-layer data, we conclude that the diffuse double layer structure at the Pt(111)-electrolyte interface deviates significantly from the Gouy–Chapman theory in the sense that the electrostatic screening is much better than predicted by purely electrostatic mean-field Poisson–Boltzmann theory.

Understanding the molecular structure of the electrode– electrolyte interface is essential in elucidating many interfacial electrochemical phenomena such as corrosion, electrocatalysis, and other charge transfer processes. The interfacial structure and composition of the electric double layer should be greatly affected by the electrostatic interactions at the interface induced by surface charging or by adsorbed species, having, for instance, a strong effect on the water structure at the interface.

Platinum is the most important and well-studied electrode material in terms of technological applications. However, the molecular structure of the electric double layer on platinum has not yet been fully resolved, partially because of the uncertainty about the location of the so-called potential of zero charge. The potential of zero charge (pzc) of a metal is the potential at which the metal surface in contact with a certain electrolyte has zero excess electronic (free) charge. According to the Gouy–Chapman (GC) theory of the electric double layer, the differential capacitance ($C_{\rm d}$) should have a minimum at the pzc, provided the pzc lies in the double layer potential window of the metal-electrolyte interface under consideration. This capacitance minimum is only observable for dilute electrolytes (ca. 10^{-3} M) because at higher concentrations the so-called inner-layer capacitance or

Helmholtz capacitance will dominate. Measurement of the GC capacitance minimum is generally considered to be the most direct observation of the pzc of a metal-electrolyte interface.

The Pt(111)-electrolyte interface is one of the most studied electrified interfaces in electrochemical surface science and in model studies of electrocatalysis. Knowing its pzc is important for a proper understanding of covalent and electrostatic interactions at this interface. Therefore many studies have aimed at measuring the pzc of Pt(111) in a nonspecifically adsorbing electrolyte such as perchloric acid. Recently, the Alicante group has concluded a value of 0.30 V (vs. SHE) based on three different methods, that is, CO displacement studies,[3,4] peroxodisulfate reduction,[5] and laser-induced temperature jump measurements of the potential of maximum entropy. [6,7] This value of the pzc of Pt(111) is also in good agreement with recent first-principles predictions.^[8] Remarkably, a GC capacitance minimum at the pzc has never been observed for Pt(111) (for a discussion, see ref. [9]).

Pajkossy and Kolb performed double layer capacitance measurements of Pt(111) in perchlorate electrolytes, but not below 0.001m concentrations. For mercury, silver and gold electrodes, 0.01m has been shown to be dilute enough to observe the GC capacitance minimum and to identify the pzc. Pajkossy and Kolb observed a capacitance maximum at 0.37 V (vs. SHE), which they initially suggested to be related to the pzc of the Pt(111) electrode. However, they reported later that the capacitance peak cannot be related to the pzc as they did not observe a capacitance minimum at the corresponding potential for low electrolyte concentration (1 mm). [10]

One issue with the reported pzc of Pt(111) of around 0.3 V (vs. SHE) is that this value of the pzc is in the double layer region only for a restricted pH range, $^{[4]}$ ca. 2–5. Given that no capacitance minimum has been observed in a 0.01M electrolyte $^{[14]}$ at pH 2, we explore here the double layer capacitance of Pt(111) in dilute non-specifically adsorbing perchlorate electrolytes at pH 3 and 4. We show the observation of the GC capacitance minimum for Pt(111) in very dilute electrolyte ($<10^{-3}\,\mathrm{M}$) at pH 4, giving a value of the pzc that agrees excellently with the pzc of Pt(111) determined by the Alicante group. By comparing to similar measurements on Au(111), we will show that the difficulty of identifying the pzc of Pt(111) by GC capacitance minimum likely lies in the anomalously large diffuse-layer GC capacitance of the Pt(111)-aqueous electrolyte interface.

Figure 1 shows the cyclic voltammetry of Pt(111) in perchlorate electrolyte (plotted as capacitance, that is, current density divided by scan rate) for pH 1 and pH 3 (with and

E-mail: m.koper@chem.leidenuniv.nl

Supporting information and the ORCID identification number(s) for the author(s) of this article can be found under: https://doi.org/10.1002/anie.201911929.

© 2019 The Authors. Published by Wiley-VCH Verlag GmbH & Co. KGaA. This is an open access article under the terms of the Creative Commons Attribution Non-Commercial License, which permits use, distribution and reproduction in any medium, provided the original work is properly cited, and is not used for commercial purposes.

^[*] K. Ojha, N. Arulmozhi, D. Aranzales, M. T. M. Koper Leiden Institute of Chemistry, Leiden University 2300 RA Leiden (The Netherlands)



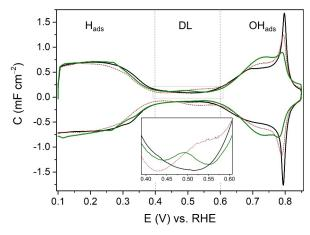
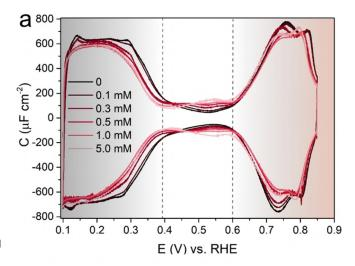


Figure 1. Cyclic voltammograms of Pt(111) in 0.1 $\,\mathrm{M}$ HClO₄ (black solid line), 1 $\,\mathrm{mM}$ HClO₄ + 99 $\,\mathrm{mM}$ KClO₄ (red dotted line) and 1 $\,\mathrm{mM}$ HClO₄ electrolyte (green solid line). Inset: the magnified version of the DL region as marked by a rectangular area. Scan rate = 10 $\,\mathrm{mVs}^{-1}$.

without added KClO₄). The voltammetry has three distinct regions, as indicated in the Figure: a hydrogen adsorption or hydrogen underpotential deposition (H_{ads}) region at $0 < E < 0.4 \, \rm V_{RHE}$; a double-layer (DL) region between $0.4 < E < 0.6 \, \rm V_{RHE}$; and an OH adsorption region between $0.6 < E < 0.85 \, \rm V_{RHE}$. The H and the OH adsorption features are reversible and shift ca. 59 mV per pH on the NHE scale, in agreement with the Nernst law. In the OH adsorption region, the Pt(111) electrode shows the characteristic "butterfly" signature [15,16] in 0.1 m HClO₄ with the ratio of OH peak intensity and the H_{UPD} \approx 2.5, which shows that the Pt(111) electrode is clean and well-ordered. The surface is also largely free from (110) and (100) steps and defects.

If the potential of zero charge is at 0.3 V vs. NHE, [5,18] then the pzc is expected at 0.36 V_{RHE} for pH 1 and at 0.48 V_{RHE} for pH 3. Therefore, only for pH 3 the pzc is in the DL window. The cyclic voltammetry for pH 3 shows an additional feature in the double layer region at $\approx 0.52-0.53$ V vs. RHE in the presence of additional KClO₄ (see the red curve in the inset in Figure 1), which was first observed by Pajkossy and Kolb, who assumed that the peak was related to the reorganization of interfacial water near the pzc.^[14] In the absence of additional salt, we do not observe a capacitance minimum in the double layer region (Figure 1), even though the pzc should be in the DL window and the 1 mm electrolyte concentration should be dilute enough given earlier results obtained with mercury, silver and gold.[11-13] Instead of a capacitance minimum, a capacitance maximum at 0.49 V vs. RHE is observed (see the green curve in the inset in Figure 1) which we assume to be related to the peak observed by Pajkossy and Kolb.^[10] Measurements to be discussed in future work show that this peak is sensitive to the nature of the electrolyte anions.

Importantly, as shown in Figure 2, a capacitance minimum is observed for a 100 μm HClO $_4$ electrolyte (pH 4) at 0.525 V vs. RHE, with the capacitance in the double layer region increasing with an increase in the ionic strength of the electrolyte. These observations are in good qualitative agreement with the GC theory, and the minimum agrees very well with the pzc of 0.30 $V_{\rm NHE}$ reported by the Alicante group.



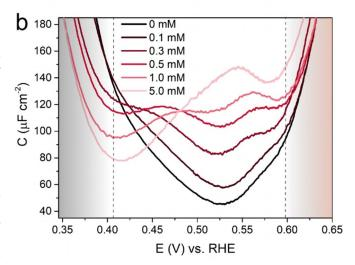


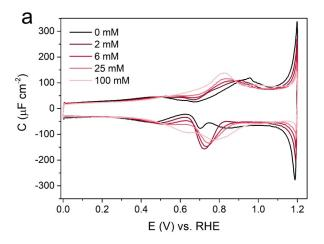
Figure 2. a) Capacitance curves obtained from the cyclic voltammograms of Pt(111) in 0.1 mm $HClO_4+xmm$ $NaClO_4$ (pH 4), the shaded areas show the H_{ads} and OH_{ads} regions. b) Magnified view of the capacitance curves in the double-layer region showing the GC capacitance minimum at the potential of zero charge at 0.53 V (vs. RHE), that is, 0.30 V vs. NHE. Scan rate = 10 mVs⁻¹.

Note that for an ionic strength of 5 mm, the capacitance curve shows a maximum, which we assume to be related to the capacitance maximum observed by Pajkossy and Kolb (the same maximum as shown in Figure 1 for pH 3). The development of the capacitance plots in Figure 2 with increasing electrolyte concentration can then be understood as a combination of an inner-layer Helmholtz capacitance with a maximum at a potential different from the pzc, and a GC capacitance with a minimum at the pzc. This may result in a "camel-shaped" capacitance plot with two maxima and one minimum for intermediate electrolyte concentrations (see the curves for 0.5 and 1 mm ionic strength).

The capacitance minimum was also observed in other non-specifically adsorbing electrolytes such as hydrofluoric acid (Figure S1 in the Supporting Information). It confirms that a ionic strength below 1 mm is needed to observe the GC capacitance minimum of Pt(111) at the pzc. To confirm the suitability of our simple CV method for capacitance measure-



ments, we also carried out similar experiments to identify the pzc of Au(111); these results are shown in Figure 3. The capacitance minimum at the pzc can be observed at higher concentrations of the electrolyte (ca. 5 mm) than for the experiments with Pt(111). These capacitance curves agree very well with those in the literature, [13] even though the conditions (primarily pH) are slightly different. The pzc of Au(111) is 0.69 V vs. RHE at pH 3 or 0.51 V vs. NHE, in good agreement with earlier reports. [19,20]



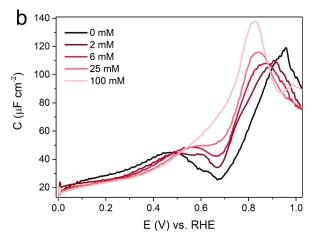


Figure 3. a) Capacitance curves obtained from the cyclic voltammograms of Au(111) in 1 mm $HClO_4+xmm$ NaClO₄ (pH 3). b) Magnified view of the capacitance curves showing the GC capacitance minimum at the potential of zero charge at 0.69 V (vs. RHE). Scan rate = 10 mV s⁻¹.

To analyze the reason why such low electrolyte concentrations are needed to observe the GC capacitance minimum on Pt(111), we perform a Parsons-Zobel (PZ) analysis, as illustrated in Figure 4. In a PZ plot, one plots the measured inverse capacitance obtained at various ionic strengths vs. the expected inverse diffuse double-layer capacitance predicted by the Gouy–Chapman theory. [21] Extrapolation to infinitely high $C_{\rm GC}$ gives the inner-layer or Helmholtz capacitance, and for the ideal electrode–electrolyte interface with the diffuse layer capacitance following the Gouy–Chapman theory, the slope of the PZ plot should be unity. Figure 4 gives the

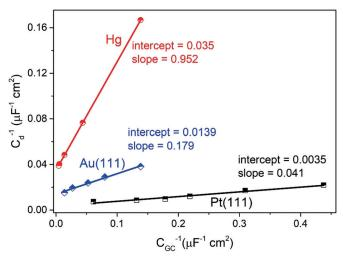


Figure 4. Parsons–Zobel plot, $1/C_d$ vs. $1/C_{GC}$: C_d values were obtained from the capacitance curves at the pzc of Pt(111) and Au(111) at various ionic strengths in Figure 2b and Figure 3b, respectively. Data for the Hg electrode were taken from ref. [22].

Parsons-Zobel plots of our data for Pt(111) and Au(111), together with the classical data of Grahame for a mercury electrode. [22] For the mercury electrode, the slope is indeed close to one, but for Au(111) and especially for Pt(111), the slope deviates very significantly from 1. According to Parsons and Zobel, specific adsorption may lead to a PZ slope smaller than 1. The significant deviation of the slope from unity in the case of Au(111) and Pt(111) suggests there are stronger ion interactions with Pt and Au compared to the Hg electrode, even though there is no evidence from the voltammetry that there is actual chemisorption of ions (as evidenced by the fact that the capacitances in perchlorate and fluoride media are very similar; see Figures 1 and S1). Another way of interpreting a PZ slope smaller than 1 is that the "real" diffuse-layer capacitance is higher than predicted by GC theory. As the GC capacitance is inversely proportional to the Debye screening length, this implies better screening (shorter Debye length) than predicted by GC theory. Basically, the double layer on Pt(111) (and to some extent also on Au(111)) is much more compact than what it should be according to GC, because the electrolyte (water + ions) interacts stronger with Pt than with Au and Hg.

Even if Figure 4 suggests that the GC capacitance is anomalously high on Pt(111) (and on Au(111) as well, though less), the linearity of the PZ plot indicates that it still scales with concentration in the same way as in the GC theory. This would imply an "effective" $C_{\rm GC}$, given by [Eq. (1)]:

$$C_{\rm GC}^{\rm M} \approx K_{\rm M} c^{1/2} \tag{1}$$

where c is the bulk concentration of the electrolyte, and $K_{\rm M}$ is a metal-dependent effective screening constant. If Equation (1) applies, the slope of the PZ plot is $K_{\rm M}^{\rm GC}/K_{\rm M}$, with $K_{\rm M}^{\rm GC}=\left(\frac{2\varepsilon_s\varepsilon_0}{k_{\rm B}T}\right)^{1/2}e_0$ for a 1:1 electrolyte, with $\varepsilon_{\rm s}$ the dielectric constant of the (interfacial) solvent, ε_0 the permittivity of vacuum, and the other symbols having their usual meaning. $^{[1,2]}$





For mercury, $K_{\rm M}$ is approximated well by the classic Gouy-Chapman theory, that is, $K_{\rm M} \approx K_{\rm M}^{\rm GC}$. For Pt(111), $K_{\rm M}$ is much higher than $K_{\rm M}^{\rm GC}$, and hence the PZ slope is much smaller than 1. Our current interpretation is that $K_{\rm M}$ expresses the accumulation of ions in the region of the outer Helmholtz plane due to specific not purely electrostatic interactions, which are not incorporated in the classic GC theory, but which apparently still scale with concentration as in GC theory. More experimental and computational work will have to reveal the correct model for the anomalously high value of $K_{\rm M}$ for Pt(111).

From Figures 2-4 it is apparent that not only the diffuselayer capacitance is higher on Pt(111) than on Au(111), but also the Helmholtz capacitance. Pt(111) has a ≈ 2 times higher inner layer capacitance than Au(111) (see the capacitance curves at 5 mm electrolyte for Pt(111) and 100 mm electrolyte for Au(111), where both do not show the GC capacitance minimum). The extrapolation from the PZ plot to zero $C_{\rm GC}^{-1}$ suggests an even larger difference. The higher inner-layer capacity suggests a higher polarizability of the interfacial water, for instance through a strong change in water orientation with electric field. Iwasita et al. observed such a change in the orientation of adsorbed water at around 0.35 V (vs. RHE) for a pH 1 solution using in situ FTIR spectroscopy, $^{[23]}$ in agreement with value of 0.30 V_{NHE} for the pzc of Pt(111). Also, the effective interfacial dielectric constant of water will be different from its bulk value, and will depend on the structure of water^[24-26] and the nature of the interface. [27] Using first-principles electronic structure calculations, Le et al. showed significant differences between the charge density distribution of interfacial water at different metal surfaces, which would lead to different inner-layer capacitances.[8]

In conclusion, we have determined the double layer properties and the potential of zero charge (pzc) of Pt(111) in perchlorate solution by identifying the Gouy-Chapman capacitance minimum. The value of $0.30~V_{\rm NHE}$ agrees very well with the value obtained by other methods. [3–7] In contrast to double-layer measurements on gold or mercury electrodes, the Gouy-Chapman capacitance minimum is only observed at electrolyte concentrations lower than 10^{-3} M, and only if the pH is between 2 and 5. In practice this means that the GC capacitance minimum can be measured only near pH 4. We stress that although the pzc of Pt(111) can only be identified at anomalously low electrolyte concentration, the value of the pzc is valid for all concentrations of perchloric acid, and hence relevant to all electrochemical experiments of Pt(111) in perchloric acid. The reason why the observation of the GC capacitance minimum of Pt(111) has remained so elusive in the past, has been partially clarified by a Parsons-Zobel analysis of the capacitance data at different ionic strengths. This analysis suggests that the "effective screening" in the diffuse part of the double layer of a Pt(111)-aqueous perchlorate interface is much better than predicted by the Gouy-Chapman theory. We hypothesize that this is related to the strong interaction of the water and the electrolyte with the Pt surface, leading to a concomitant distribution (accumulation) of ions that does not follow a purely electrostatic mean-field Poisson-Boltzmann distribution. Our result lavs the foundation for a detailed exploration of interfacial phenomena at the Pt-electrolyte interface, contributing to a more in-depth understanding of the reactivity of this important interface.

Experimental Section

Electrochemical investigations were performed at room temperature on a Bio-Logic VSP300 potentiostat, in a three-electrode setup where a Pt(111) single crystal bead (area = 0.08 cm^2), a Pt wire and an internal Reversible hydrogen electrode (RHE) were used as working, counter and reference electrode, respectively. The Pt(111) crystal was grown and polished by following the procedure as described in Arulmohzi et al. [28,29] Experiments were performed in a standard glass cell, except for measurements using hydrofluoric acid, which were carried out in a fluorinated ethylene propylene (FEP, Nalgene) electrochemical cell. All glassware was cleaned in a mixture of H₂SO₄ and potassium permanganate overnight, followed by rinsing with a mixture of H₂SO₄ and H₂O₂. Before use, the glassware was rinsed and boiled several times with ultrapure water. Prior to each measurement, the Pt(111) single crystal was flame annealed and cooled down to room temperature in an Ar:H₂ (4:1) environment.^[30] Subsequently, the crystal was protected with a drop of water saturated with the same gas mixture and transferred to the electrochemical cell. The electrochemical measurements were performed with the singlecrystal electrode in hanging meniscus configuration. All the experiments were performed by first acquiring a blank voltammogram of the Pt(111) in the 0.1M HClO₄ electrolyte solution purged with Ar (Linde Gas, HiQ Ar 6.0) to ensure the cleanliness and order of both the cell and the electrode. During the measurement, an Ar blanket above the electrolyte was created to avoid interference of oxygen from air. Afterwards, all the measurements were done in the appropriate perchlorate electrolyte purged with Ar. The capacitance curves were obtained by voltammetry at low scan rate (10 mV s⁻¹) and dividing the current density by the scan rate. The high solution resistance of the diluted electrolytes was corrected using IR compensation. The capacitance values obtained in this way agree very well with literature capacitance values obtained by impedance measurements.[10,13,14] Electrolytes were made from ultrahigh pure water (Milli-Q, 18.2 MΩcm), high purity reagents HClO₄ (60% Suprapur, Sigma), NaClO₄ (99.99 %, Sigma), NaF (99.99 %, suprapur, Millipore, Germany) and HF (40%, suprapur, Sigma).

Acknowledgements

This work received partial support by Hitachi Ltd. and Hitachi High-Technologies Corporation. The research of D.A. is supported by Tata Steel Nederland Technology B.V. through the Materials Innovation Institute M2i and the Technology Foundation TTW, which is the applied science division of the Netherlands Organization for Scientific Research (NWO) and the Technology Programme the Ministry of Economic Affairs of the Netherlands.

Conflict of interest

The authors declare no conflict of interest.

Keywords: double layer capacitance · Gouy– Chapman capacitance · metal–electrolyte interface · potential of zero charge · Pt(111)

Communications





How to cite: Angew. Chem. Int. Ed. 2020, 59, 711–715 Angew. Chem. 2020, 132, 721–725

- [1] A. J. Bard, L. R. Faulkner, *Electrochemical Methods Fundamentals and Applications*, Wiley, Hoboken, **2001**.
- [2] W. Schmickler, E. Santos, *Interfacial Electrochemistry*, Springer, Berlin, Heidelberg, 2010.
- [3] R. Gómez, V. Climent, J. M. Feliu, M. J. Weaver, J. Phys. Chem. B 2000, 104, 597-605.
- [4] R. Rizo, E. Sitta, E. Herrero, V. Climent, J. M. Feliu, *Electro-chim. Acta* 2015, 162, 138–145.
- [5] R. Martínez-Hincapié, V. Climent, J. M. Feliu, Electrochem. Commun. 2018, 88, 43-46.
- [6] R. Martínez-Hincapié, P. Sebastián-Pascual, V. Climent, J. M. Feliu, Russ. J. Electrochem. 2017, 53, 227 236.
- [7] P. Sebastián, R. Martínez-Hincapié, V. Climent, J. M. Feliu, Electrochim. Acta 2017, 228, 667–676.
- [8] J. Le, M. Iannuzzi, A. Cuesta, J. Cheng, Phys. Rev. Lett. 2017, 119, 016801.
- [9] A. Cuesta, Surf. Sci. 2004, 572, 11-22.
- [10] T. Pajkossy, D. M. Kolb, Electrochem. Commun. 2003, 5, 283–285.
- [11] D. C. Grahame, Chem. Rev. 1947, 41, 441 501.
- [12] G. Valette, J. Electroanal. Chem. 1989, 269, 191-203.
- [13] J. Lecoeur, A. Hamelin, C. R. Acad. Sci. Ser. C 1974, 279, 1081 1084.
- [14] T. Pajkossy, D. M. Kolb, *Electrochim. Acta* **2001**, *46*, 3063 3071.
- [15] M. L. Lynch, B. J. Barner, R. M. Corn, J. Electroanal. Chem. 1991, 300, 447–465.

- [16] M. T. M. Koper, J. J. Lukkien, J. Electroanal. Chem. 2000, 485, 161–165.
- [17] V. Climent, R. Gómez, J. M. Orts, J. M. Feliu, J. Phys. Chem. B 2006, 110, 11344–11351.
- [18] R. Martínez-Hincapié, V. Climent, J. M. Feliu, Curr. Opin. Electrochem. 2019, 14, 16–22.
- [19] D. M. Kolb, *Prog. Surf. Sci.* **1996**, *51*, 109–173.
- [20] U. W. Hamm, D. Kramer, R. S. Zhai, D. M. Kolb, J. Electroanal. Chem. 1996, 414, 85–89.
- [21] R. Parsons, F. G. R. Zobel, *J. Electroanal. Chem.* **1965**, *9*, 333 348.
- [22] D. C. Grahame, J. Am. Chem. Soc. 1954, 76, 4819 4823.
- [23] T. Iwasita, X. Xia, J. Electroanal. Chem. 1996, 411, 95-102.
- [24] S. Evans, J. Glaciol. 2017, 773-789.
- [25] J. L. Aragones, L. G. MacDowell, C. Vega, J. Phys. Chem. A 2011, 115, 5745 – 5758.
- [26] M. E. Hobbs, M. S. Jhon, H. Eyring, Proc. Natl. Acad. Sci. USA 1966, 56, 31–38.
- [27] D. J. Bonthuis, S. Gekle, R. R. Netz, Phys. Rev. Lett. 2011, 107, 166102.
- [28] N. Arulmozhi, G. Jerkiewicz, Electrocatalysis 2016, 7, 507-518.
- [29] N. Arulmozhi, G. Jerkiewicz, Electrocatalysis 2017, 8, 399-413.
- [30] N. Arulmozhi, D. Esau, J. van Drunen, G. Jerkiewicz, *Electro-catalysis* 2018, 9, 113–123.

Manuscript received: September 18, 2019 Revised manuscript received: October 30, 2019 Accepted manuscript online: November 4, 2019 Version of record online: November 26, 2019